Available online at www.sciencedirect.com
ScienceDirect
Journal of Hazardous Materials 156 (2008) 23–35
Journal of Hazardous Materials
www.elsevier.com/locate/jhazmat

Removal of heavy metals from acid mine drainage (AMD) using coal fly ash, natural clinker and synthetic zeolites

C.A. Ríos [a,b,*], C.D. Williams [b], C.L. Roberts [b]

[a] *Escuela de Geología, Universidad Industrial de Santander, A.A 678, Bucaramanga, Colombia*
[b] *School of Applied Sciences, The University of Wolverhampton, Wulfruna Street, Wolverhampton WV1 1SB, UK*

Received 31 August 2007; received in revised form 21 November 2007; accepted 28 November 2007
Available online 14 December 2007

Abstract

Acid mine drainage (AMD) is a widespread environmental problem associated with both working and abandoned mining operations, resulting from the microbial oxidation of pyrite in presence of water and air, affording an acidic solution that contains toxic metal ions. The generation of AMD and release of dissolved heavy metals is an important concern facing the mining industry. The present study aimed at evaluating the use of low-cost sorbents like coal fly ash, natural clinker and synthetic zeolites to clean-up AMD generated at the Parys Mountain copper–lead–zinc deposit, Anglesey (North Wales), and to remove heavy metals and ammonium from AMD. pH played a very important role in the sorption/removal of the contaminants and a higher adsorbent ratio in the treatment of AMD promoted the increase of the pH, particularly using natural clinker-based faujasite (7.70–9.43) and the reduction of metal concentration. Na-phillipsite showed a lower efficiency as compared to that of faujasite. Selectivity of faujasite for metal removal was, in decreasing order, Fe > As > Pb > Zn > Cu > Ni > Cr. Based on these results, the use of these materials has the potential to provide improved methods for the treatment of AMD.

Keywords: Acid mine drainage; Mining industry; Sorption; Removal; Heavy metals; Ammonium; Sorbents

1. Introduction

Wales (United Kingdom) is particularly rich in mineral resources, the type and distribution of which are related to the complex geologic and tectonic history. The Parys Mountain copper–lead–zinc deposit of Anglesey (North Wales) represents a volcanogenic massive sulphide (VMS) district of major metallogenic importance, which is characterized by the occurrence of concordant massive to banded sulphide lens formed by volcanic processes normally on the sea floor. The Great Opencast (Fig. 1(a)) was opened up at an early stage of mining and forms part of the geological heritage of Parys Mountain, being focus of tourism attraction for visitors due to its similarity with a lunar landscape. However, mining activities at this deposit have generated AMD, which results as a consequence of a complex series of geochemical reactions that occur when sulphide minerals are exposed to the atmosphere under an oxidising environment, producing polluted waters strongly acidic with high concentrations of iron, sulphate and toxic metals, responsible for the resulting damage to health of aquatic flora and fauna. Although AMD is naturally occurring, underground and open pit mining activities may greatly accelerate its production because they expose fresh iron and sulphide surfaces to oxygen. Predictions of the future loading of dissolved metals from inactive mine sites suggest that sulphide oxidation and the release of dissolved metals will continue for decades to centuries [1]. Estimated costs for stabilization of these sites are in the billions of dollars [2].

Iron sulphide minerals, especially pyrite (FeS_2), contribute the most to formation of AMD. The pyrite oxidation process has been extensively studied and can be summarized by the following reaction sequence:

$$FeS_2 + 3.5O_2 + H_2O \rightarrow Fe^{2+} + 2SO_4{}^{2-} + 2H^+ \quad (1)$$

$$4Fe^{2+} + O_2 + 4H^+ \rightarrow 4Fe^{3+} + 2H_2O \quad (2)$$

$$4Fe^{3+} + 12H_2O \rightarrow 4Fe(OH)_3(s) \downarrow + 12H^+ \quad (3)$$

$$FeS_2 + 14Fe^{3+} + 8H_2O \rightarrow 15Fe^{2+} + 2SO_4{}^{2-} + 16H^+ \quad (4)$$

* Corresponding author at: School of Applied Sciences, The University of Wolverhampton, Wulfruma Street, Wolverhampton WV1 1SB, UK.
Tel.: +44 1902 322679; fax: +44 1902 322714.
E-mail address: C.A.RiosReyes@wlv.ac.uk (C.A. Ríos).

0304-3894/$ – see front matter.
doi:10.1016/j.jhazmat.2007.11.123

Fig. 1. (a) A panoramic view of the Great Opencast of the Parys Mountain copper–lead–zinc deposit, Anglesey (North Wales), which can be obtained from the viewing platform; (b) brick-lined precipitation ponds used to extract copper; (c) and (d) shallow and deep transient ponds from rainfall between spoil heaps near to the top of the mountain and by the entry road of the copper mine, respectively.

During the first step, pyrite reacts with oxygen and water, producing Fe^{2+} and sulphuric acid by reaction (1). The second step involves the oxidation of Fe^{2+} to Fe^{3+} by reaction (2), which is pH-dependent. The third step corresponds to the hydrolysis of Fe^{3+} with water to form a ferric hydroxide precipitate (ferrihydrite) and the release of additional acidity, which is promoted by the pH-dependent reaction (3). The fourth step is defined as the oxidation of additional pyrite by Fe^{3+} according to reaction (4). The pyrite oxidation is controlled by bacterial species that have definite pH growth range and pH growth optimum [3]. The conversion of Fe^{2+} to Fe^{3+} in the overall pyrite reaction sequence has been described as the 'rate determining step' [4], which can be greatly accelerated by bacterial action. In AMD there are many mineral-degrading acidophiles involved in the metabolism of pyrite and the metabolic pathways involved in this process are pyrite dissolution, iron oxidation, iron reduction, and sulphur oxidation [3]. The most common pyrite-oxidizing bacterium is *Acidithiobacillus ferrooxidans*, which is of great practical importance due to the extensive acid and metal pollution generated when this species releases metals from acid mine waters [5]. Once pyrite oxidation and acid production has begun, conditions are favourable for bacteria to further accelerate the reaction rate. At pH values of about 6 and above, bacterial activity is thought to be insignificant or comparable to abiotic reaction rates. The knowledge of the mineralogical processes occur during the atmospheric oxidation of pyrite and other sulphide minerals in the presence of oxidising bacteria and any other product generated as a consequence of oxidation reactions (e.g., heavy metals solubilised by acid solutions) is very useful in both the prediction of AMD and its treatment. Traditionally, the treatment of AMDs consists in the neutralization with limestone ($CaCO_3$) or similar materials, resulting in the precipitation of Fe and other metal hydroxides as well as also gypsum ($CaSO_4$). AMD treatment with limestone can increase the pH to 6.0–7.5 [6], allowing the metals to be removed from solution. Several procedures for AMD treatment have been developed [7–17], although adsorption has been the preferred method for heavy metal removal, because it is considered a particularly effective technique. There are two general categories of AMD treatment which are well investigated: (1) active treatment, which requires the use of chemical treatment systems to buffer acidity, and (2) passive treatment, which allows naturally occurring chemical and biological processes to do the work in a controlled system outside of the receiving polluted effluent. However, AMD remediation can be very costly and difficult due to the high costs of activated carbon's production and regeneration for water treatment. Therefore, alternative low-cost liming substitutes are constantly sought. Such adsorbents should be readily available, economically feasible and easily regenerated. Coal fly ash (CFA) has been used for reclamation, asphalt shingle production, quarry-fill and sludge stabilization, but most is disposed as landfill. Due to the shortage of landfill sites and stricter environmental regulation, new ways to recycle this coal combustion by-product should be quickly developed, and one new way is through its zeolitization. The potential use of CFA, as well as the synthetic zeolites based on this solid

waste material, in water purification has been evaluated by a number of research groups and the removal of heavy metals from contaminated water has been studied extensively [18–22]. Moreover, recent works showed that the addition of CFA to a mining residue from the Iberian Pyrite Belt resulted in acid neutralization, metal retention in neoformed precipitates, and therefore, the improvement of the leachates' quality [23]. In these conditions, Fe-precipitation as a coating on pyrite surfaces (microencapsulation technology) may prevent interaction between oxidizing agents and pyrite grains, thus halting pyrite oxidation and AMD production [24]. To our knowledge, no previous effort has been made to use natural clinker (NC) or the synthesis products obtained from this material as sorbents in water treatment. The aim of the present study is to examine at laboratory-scale the effectiveness of CFA, NC and synthetic zeolites as sorbents in removing Cu, Pb, Zn, Ni, Cr, Fe and As from AMD generated at the Parys Mountain copper–lead–zinc deposit.

2. Materials and methods

2.1. Sampling sites

The surface drainage waters at Parys Mountain are strongly acidic (pH < 2) and metal-rich due to the oxidation of sulphide minerals, and its orange-brown colour is due to the very high concentrations of ferric iron in solution. AMD samples were collected in three major locations from the abandoned copper–lead–zinc deposit and sealed in high-density polyethylene bottles. On-site analyses of the pH and electrical conductivity and temperature were performed in different surface drainage waters. Brick-lined precipitation ponds (Fig. 1(b)) have been used to extract copper from water which was pumped up to the mountain top and allowed to drain down through the spoil and underground workings, dissolving copper from the rocks on the way. The copper precipitation is carried out by the accumulation of copper-rich water in these ponds and then adding scrap iron, which results in dissolution of iron and precipitation of copper as a black powder, that can be removed for processing. This process has been very efficient to recover small amounts of relatively pure copper. Fig. 1(c) illustrates a shallow transient pond from rainfall occurring between spoil heaps near to the top of the mountain. Fig. 1(d) shows a deeper transient pond located by the entry road of the copper mine, where the lowest pH (1.69) was obtained.

2.2. Sorbents

For the treatment of AMD, CFA, NC and synthetic zeolites were used as sorbents. CFA is a waste incineration by-product supplied by the Rugeley Power Station, West Midlands (England), which is generated by pulverized coal combustion (PCC) and classified as Class F fly ash. NC is a product of coal-bed fires ignited by natural processes obtained from the late Paleocene Cerrejón Formation, Cerrejón coal deposit, Colombia. Synthetic zeolites were prepared by two methods: (1) classic hydrothermal synthesis using NC and (2) alkaline fusion prior to hydrothermal synthesis using both CFA and NC. In the first method, sodium hydroxide pellets were added to distilled water to prepare a 1 M NaOH solution. Then, NC was added to the alkaline solution with a solution/raw material ratio of 3.06 ml/g. The progressive addition of reagents was carried out under stirring conditions until dissolve them to homogenize the reaction gels. In the second method, sodium hydroxide powder was dry mixed with CFA or NC (alkaline activator/raw material ratio of 1.2) for 30 min and the resultant mixture was fused at 600 °C for 1 h. The alkaline-fused products were dissolved in water (H_2O/alkali fused raw material ratio = 4.89 ml/g), with stirring for 3.5 h until the hydrogels were homogenized. The hydrogels were transferred to PTFE bottles of 200 ml and heated under static conditions at 100 °C for 72 h (first method) or 60 °C for 24 h (second method). pH was measured before and after hydrothermal treatment. The reactors were removed from the oven at the scheduled reaction times and were quenched in cold water. After hydrothermal treatment, the reaction mixtures were filtered and washed with distilled water and the synthesis products were oven dried at 80 °C. The alkaline fusion step of the starting materials with NaOH was useful to produce as far as possible, a highly crystalline homoionic Na-form faujasite type zeolite and its subsequent application in decontamination experiments. The reagents used to activate the starting materials for zeolite synthesis were sodium hydroxide, NaOH, as pellets (99%, from Aldrich Chemical Company Inc.) or powder (96%, from BDH GPR) and distilled water using standard purification methods.

2.3. Characterization of sorbents

The mineral phases in sorbents were studied by X-ray diffraction (Philips PW1710 diffractometer) operating in Bragg–Brentano geometry with Cu-Kα radiation (40 kV and 40 mA) and secondary monochromation. Data collection was carried out in the 2θ range 3–50°, with a step size of 0.02°. Phase identification was made by searching the ICDD powder diffraction file database, with the help of JCPDS (Joint Committee on Powder Diffraction Standards) files for inorganic compounds. A ZEISS EVO50 scanning electron microscope, equipped with an energy dispersive (EDX) analyser, was used for microstructural characterization, under the following analytical conditions: I probe 1 nA, EHT = 20.00 kV, beam current 100 μA, Signal A = SE1, WD = 8.0 mm.

2.4. Batch experiments and water analyses

The sorption of Cu, Pb, Zn, Ni, Cr, Fe, As and ammonium onto coal fly ash, natural clinker and synthetic zeolites was studied in laboratory batch experiments, which were carried out at room temperature to investigate the efficiency of the sorbents for removing heavy metals and ammonium from AMD. A weighted amount of sorbent (0.25 and 1 g) was introduced in PVC plastic bottles of 100 ml, and then a volume of 20 ml of AMD with pH 1.96 was added. Later, the sorbent:AMD mixtures were continuously shaked between 5 min and 24 h, and the temporal evolution of the solution pH and EC was monitored. At each scheduled reaction time the PVC plastic bottles were removed from the

shaker and the adsorbents were separated by filtration, while the filtrates were stored at 4 °C in a refrigerator for chemical analyses. All measurements were done according to the Standard Methods for the Examination of Water and Wastewater. The pH and electrical conductivity of the raw AMD and the filtrates obtained after batch experiments were measured using a pH 211 Auto-calibration bench pH/mV meter (Hanna instruments) and a Cond 315i conductivity meter (WTW instruments), respectively. The metal concentrations were determined using a Spectro Ciros ICP-AE Spectrometer. A Photometer 7100 fully integrated with the Palintest water test system was used to measure ammonia over the ranges 0–1.0 mg/l N. Dilutions were made using distilled water depending on the original EC of each sample.

3. Results and discussion

3.1. Characterization of sorbents

Fig. 2 illustrates the XRD patterns and SEM microphotographs of the different sorbents used in this study. Elemental composition data for the raw materials and synthesis products are shown in Table 1. CFA mainly consists of an amorphous phase giving rise to the broad hump between 20° and 35° 2θ and the primary crystalline phases are quartz and mullite as identified by the sharp peaks (Fig. 2(a)), which were produced during the thermal decomposition of clay minerals such as kaolinite during coal combustion. This residue from the combustion of coal has ≥70% of $SiO_2 + Al_2O_3 + Fe_2O_3$, with a SiO_2/Al_2O_3 ratio = 1.21, and very low contents of Fe, Ca and S. Therefore, it can be classified as a low-calcium Sialic Class F CFA, which is commonly produced from the burning of higher-rank bituminous coals and anthracites [25]. Fig. 2(a) reveals that the particles of CFA are predominantly spherical in shape with a relatively smooth surface texture (0.25–40 μm). The spherical particles are generally hollow and empty (cenospheres) but some of them contain smaller spheres in their interiors (plerospheres). NC represents a geomaterial with a complex chemistry and mineralogy, which makes it difficult to do quantitative analysis by conventional X-ray diffraction. Quartz is the dominant mineral phase and weak peaks indicate the occurrence of hematite, muscovite and anatasa (Fig. 2(b)). NC contains very high contents of SiO_2 and Al_2O_3, with a SiO_2/Al_2O_3 ratio = 2.40, with very low contents of major impurities, such as Ca and S, and a higher content of Fe associated with the presence of hematite that can show an inert behaviour. It shows a blocky-like shape with vitreous amorphous material as shown in Fig. 2(b), with a particle size of 1–150 μm. The SiO_2/Al_2O_3 ratios of 1.21 and 2.40 of CFA and NC, respectively, are appropriate for the synthesis of low-Si zeolitic materials with high cation exchange capacity. Fig. 2(c) and (d) illustrate the X-ray diffraction patterns of CFAF and NCF, respectively, obtained via alkaline fusion of the raw materials followed by hydrothermal treatment at 100 °C for 24 h, which are characterized by the disappearance of the characteristic peaks of the raw materials, although faujasite crystallized along with hydroxysodalite when NC was used as starting material. The characteristic morphology of CFAF is illustrated in Fig. 2(c) as single large bipyramidal crystals, which have grown at the expense of an intergrowth of cubic polycrystals of CFAF. Fig. 2(d) shows the occurrence of octahedral crystals of NCF that are being transformed to a more stable phase such as hydroxysodalite (aggregates of bladed crystals growing onto the surface of faujasite) that can be attributed to excessive enrichment of NCF with the alkaline activator (NaOH) [26]. Fig. 2(e) shows the X-ray diffraction pattern and the morphology of Na-phillipsite, which represent the main zeolitic phase obtained after activation of NC by the conventional hydrothermal treatment. Na-phillipsite crystallized along with traces of hydroxysodalite and relic quartz and is characterized by large clusters of radiating tetragonal prisms. The morphology of the treated raw materials is represented by very fine grain size particles (0.25–5 μm), which crystallized as aggregates of many zeolite crystals onto the original surface of the CFA and NC particles, indicating a larger surface area of the zeolitic products due to their smaller particle size compared with that of the raw materials. Crystal size and morphology are important to constrain the sorption properties of the sorbents with potential as ion exchangers in water treatment, taking into account that the reactivity of the sorbents and extent and mode of metal uptake onto sorbents which appear to be largely dependent on crystal size and morphology.

Table 1
Chemical composition of the adsorbents

Composition (wt%)	CFA	NC	CFAF	NCF	NCZ
SiO_2	52.96	56.60	33.81	49.08	58.75
Al_2O_3	43.60	23.61	38.28	27.67	24.31
Fe_2O_3	0.41	9.41	0.78	1.75	7.55
MgO	0.33	3.94	0.00	0.00	0.00
K_2O	1.30	1.95	0.00	0.66	3.64
Na_2O	0.33	1.41	15.76	20.85	4.23
CaO	0.48	0.53	10.04	0.00	0.43
MnO	0.00	0.35	0.00	0.00	0.00
TiO_2	0.14	1.10	1.33	0.00	1.09
SO_3	0.45	1.11	0.00	0.00	0.00
SiO_2/Al_2O_3 ratio	1.21	2.40	0.88	1.77	2.42

CFA, coal fly ash; NC, natural clinker; CFAF, coal fly ash-based faujasite; NCF, natural clinker-based faujasite; NCZ, natural clinker-based Na-phillipsite.

Assessment of the results presented in Table 1 shows that in general the weight percent of the major oxides have been reduced during zeolite synthesis, which was expected, with some exceptions. After the synthesis process, the raw materials incorporated significant amount of Na due to their activation with NaOH, although CFAF and NCF showed higher Na contents. Fe content decreased after activation of natural clinker, particularly using the alkaline fusion approach, whereas Ca content increased after activation of CFA. The SiO_2/Al_2O_3 ratio has a very significant impact on the zeolite performance in the decontamination process, since according to Misak [27] generally a zeolite with a low SiO_2/Al_2O_3 ratio will tend to be hydrophilic, while a high silica zeolite (>2.00) will tend to be hydrophobic and organophillic. CFAF and NCF showed lower SiO_2/Al_2O_3 ratios, varying from 0.88 to 1.77, than those of the starting materials and NCZ showed a similar ratio to that obtained

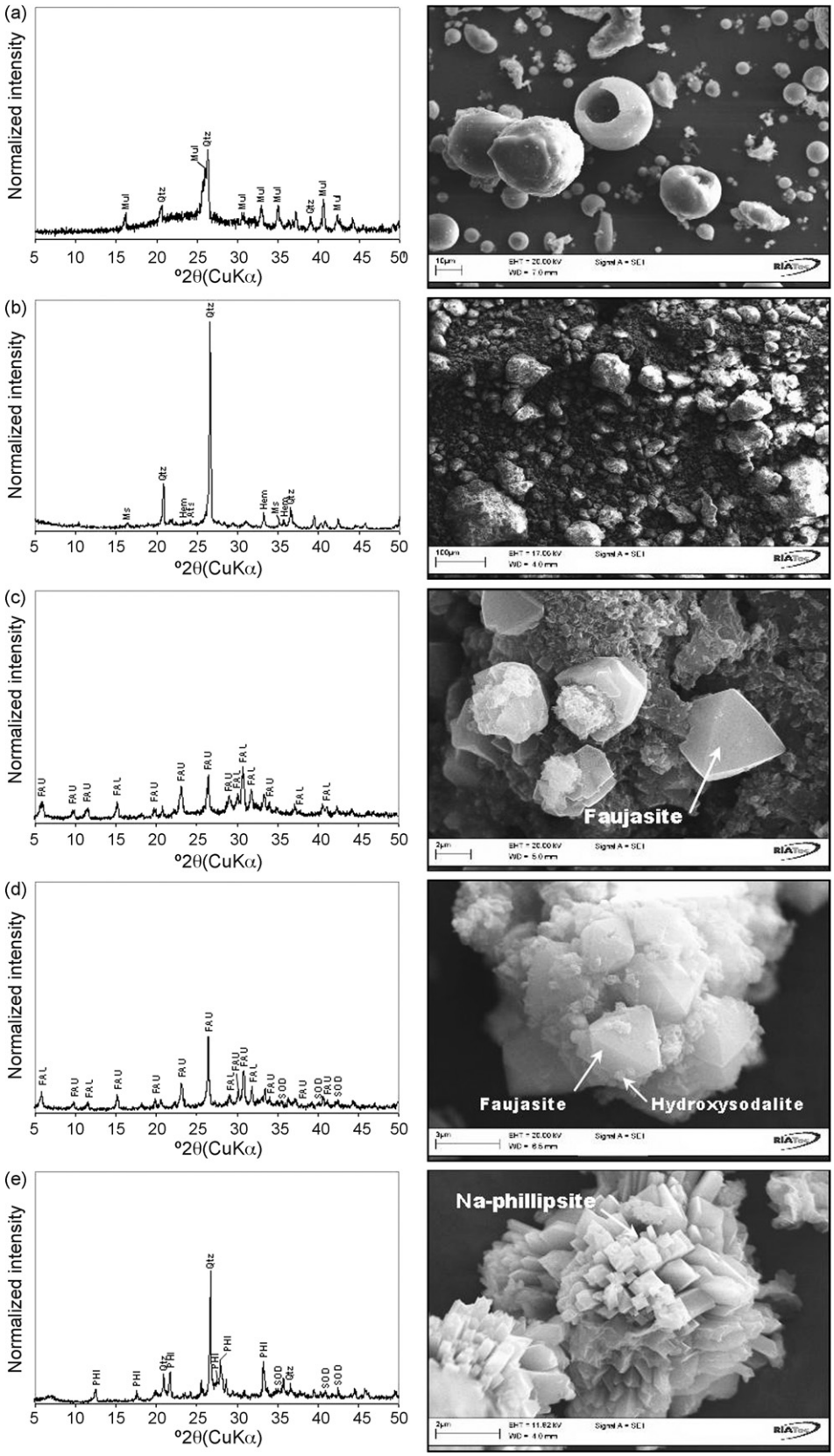

Fig. 2. XRD patterns (left) and SEM microphotographs (right) of CFA (a), NC (b), CFAF (c), NCF (d) and NCZ (e). FAU, faujasite; PHI, Na-phillipsite; SOD, hydroxysodalite; Qtz, quartz; Mul, mullite; Ms, muscovite; Hem, hematite; Ats, anatase.

for the raw material. Therefore, based on the low SiO_2/Al_2O_3 ratios determined in the as-synthesized faujasite, the expected results would be a higher concentration of terminal Al–OH species at the zeolite–water interface during the batch reaction, as well as increased hydrophilic nature of the zeolite and subsequent enhanced metal exchange capacity. However, although the cation exchange capacity of zeolites represents a very important characteristic quality in the removal of undesired species from polluted effluents, it is not the deciding factor in determination of the zeolite's performance during ion exchange processes, since numerous other factors also needs to be considered [28].

3.2. Characterization of AMD samples

At Parys Mountain, there is very little detectable change in water chemistry along the surface drainage waters, where AMD was collected. Field data of AMD for 19 July 2007 were: pH between 1.69 and 1.99; electrical conductivity between 9.27 mS/cm (22.3 °C) and 3.89 mS/cm (21.0 °C) and ammonium concentration 7.0 mg/l. Lab data of AMD for 20 July 2007 were: pH between 1.96 and 2.07; electrical conductivity between 9.97 mS/cm (16.0 °C) and 5.05 mS/cm (17.0 °C) and ammonium concentration 3.0 mg/l. AMD was strongly acidic and contained significant levels of metal ions, especially Fe, and sulphate. The acidic characteristic of the AMD results from the percolation of water through sulphide minerals, generally pyrite, which oxidizes and dissociates when in contact with air and water. Therefore, Fe^{2+} is released and rapidly oxidizes to Fe^{3+}, which precipitates as hydroxides. After the onset of the reaction, a cyclic series of events takes place starting with the oxidation of Fe^{2+} to Fe^{3+} that is subsequently reduced by pyrite, releasing Fe^{2+} which increases the acidity of the solution [29]. Alternatively other metals like Zn, Cu and minor Pb and As occurring in minerals associated to the volcanic-hosted massive Zn–Pb–Cu sulphide mineralization, can be solubilised and lixiviated as a consequence of the characteristic acidity of the water and, therefore, the concentration of these elements is often high. On the other hand, Smith et al. [30] investigated the relationship between iron bacteria type, abundance, stream environment and water/sediment chemistry in AMDs and concluded that bacteria exert a strong control over the precipitation of Fe–Mn oxyhydroxides, which can attenuate the concentration of metal ions by sorption and coprecipitation processes. AMD characterization indicates that the effluents at Parys Mountain were highly toxic to organisms and could destroy the natural ecosystem when disposed without previous treatment.

3.3. AMD treatment using CFA, NC and synthetic zeolites

The main objective of this experimental work was to carry out a study of the sorption efficiency of both the raw starting materials used in zeolite synthesis and their as-synthesized products, with respect to the immobilization of heavy metals and ammonium and to explore the applicability of these low-cost ion exchangers for the decontamination of AMD.

3.3.1. Kinetics of the neutralization reaction

Neutralization is generally the first step in AMD treatment. Therefore, the kinetics of the neutralization reaction was investigated by monitoring the pH and electrical conductivity of sorbent:AMD mixtures (0.25 g/20 ml and 1 g/20 ml) over a period of 24 h. Figs. 3(a) and (b) show the pH and electrical conductivity trends, respectively, for the neutralization reactions between the investigated sorbents and the AMD (0.25 g/20 ml). A small increase of the initial pH (1.96) of the AMD occurred on contact with CFA (2.54) and NC (2.42) and synthesis products (2.99–3.40) within the first 5 min of shaking. The reaction rates decrease as equilibrium is approached. pH can increase as a consequence of the progressive dissolution of the sorbent during the shaking process, and it can decrease due to the release of relict organic matter. The pH was stabilized within 1 h when the CFA and NC were reacted with AMD, whereas 2 h were required using the synthetic zeolites as sorbents. The final pH ranges from 1.86 to 2.66 (raw materials) to 2.86–4.42 (synthesis products), being higher when faujasite was used. No breakthrough to alkaline pH was observed, which indicates that contact time did not affect the alkalinity using a dosage of 0.25 g, but using a higher sorbent ratio a strong change in pH was observed as will be discussed later. The lack of buffering capacity for the solution can be attributed to the very low concentration of Fe^{3+}/Fe^{2+}, Al^{3+}, Mn [31]. A buffering region is associated to oxidation and hydrolysis of Fe^{2+} with releases H^+ ions and delays rise in pH [32]. Electrical conductivity ranges of 5.00–6.93 mS/cm and

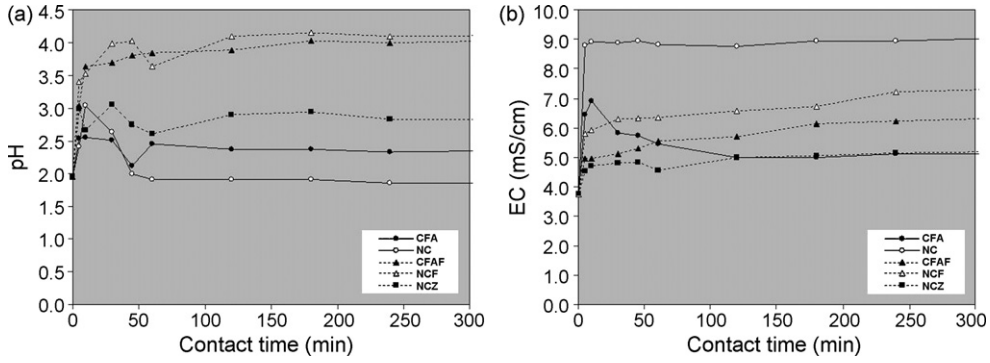

Fig. 3. pH (a) and electrical conductivity (b) variation as a function of time during the sorption batch experiments with starting pH of 1.96 and EC of 3.77 mS/cm, sorbent dosage of 0.25 g, and volume of AMD of 20 ml.

8.76–10.38 mS/cm were obtained for the CFA and NC, respectively, whereas the as-synthesized products showed electrical conductivity ranges of 4.96–7.74 mS/cm, 5.80–8.63 mS/cm and 4.53–5.87 mS/cm. A sudden increase in electrical conductivity was observed during the first 5 min for all batch experiments, indicating that very soluble material dissolved very quickly resulting in a rapid and irregular increase in electrical conductivity during the initial contact sorbent:AMD. After 1 h of reaction, the electrical conductivity values maintained fairly stable for the rest of the time intervals when NC was used. On the other hand, CFA showed a regularly and systematically decrease in electrical conductivity, which can be associated to a reduction in sulphate accompanied by the formation gypsum, whereas the use of zeolitic products promoted a progressively increase in electrical conductivity, although showing slight concentration fluctuations. After an initial very rapid increase in electrical conductivity, the release of solutes to the solution slows down during further reaction. Therefore, it is possible that ions from acid-generating and acid-neutralizing reactions can effectively increase both the salt concentration (salinity) of the AMD and its electrical conductivity, which means that the sorbents released species in solution.

3.3.2. Ammonium removal

The removal of ammonium from AMD using the raw materials and synthesis products is illustrated in Fig. 4(a) for a sorbent:AMD mixture of 0.25 g/20 ml. CFA produced an increase in ammonium after 10 min, which becomes stable between 10 and 30 min and then abruptly decreases to the lower concentration, although it shows a strongly reversal character. CFA seems to release ammonium after some time in contact with AMD, which has been observed in similar studies [22]. NC produced more or less stable behaviour in ammonium trend during the first hour of contact time, and then it shows a small increase between 1 and 3 h, followed by a gradual small decrease between 3 and 24 h. CFAF and NCF show an increase in ammonium after 5 or 10 min and then it abruptly decreases to lower concentrations, becoming stable after 30 min. NCZ produced a small increase in ammonium after 5 min and then it decreases after 10 min. However, the ammonium concentration shows a strongly reversal character. On the other hand, the synthesis products show a capacity to adsorb ammonium which could be mainly through ion-exchange.

3.3.3. Heavy metal removal

The immobilization of heavy metal ions from aqueous solutions is quite a complicated process, consisting of ion exchange and adsorption and is likely to be accompanied by precipitation of metal hydroxide complexes on active sites of the particle surface [33]. The removal of heavy metals from AMD using the raw materials and as-synthesized zeolites is illustrated in Fig. 4(b)–(h) for a sorbent:AMD mixture of 0.25 g/20 ml. As shown in Fig. 4(b), Ni increased within the first 5 min, decreasing between 5 and 10 min when the raw materials were used, whereas steep and slight increases were observed using faujasite (CFAF and NCF) and NCZ. All sorbents produced a progressive increase between 10 and 45 min, although CFA and NC showed a steep increase at 45 min and 1 h, respectively. During the first hour of reaction, all sorbents produced inconsistent trends characterized by concentration fluctuations and a reversible behaviour. After 2 h, NC and NCZ produced a progressive increase and decrease in Ni concentration, respectively. However, the concentration of this metal ion tends to increase at longer reaction times.

In general, Cr (Fig. 4(c)) displays very low concentrations, which tend to stabilize after sorbent:AMD reaction, except when CFA was used, although no complete removal of Cr was reached. The addition of CFA to AMD produced a steep increase in Cr, within the first 5 min, followed by a decrease between 5 and 10 min. Then a progressive increase was observed between 10 and 45 min, followed by a new decrease up to 2 h, showing a slight progressive increase with reaction time. Cr concentrations after CFA–AMD interaction are higher than those contained originally in the raw AMD. This is due to the fact that CFA releases Cr during its dissolution. NC also produced very low concentrations of Cr, with significant fluctuations, particularly at 1 h. When synthesis products were used, lower residual concentrations of Cr were obtained, although with an inconsistent behaviour of their trends. CFAF and NCF produced similar trends, with a decrease in Cr within the first 10 min, slightly increasing up to 3 h, decreasing again between 3 and 4 h, after which it stabilized. The lowest residual concentrations were observed after 4 h using NCF and NCZ.

Pb (Fig. 4(d)) showed a steep decrease during the first 5 min using CFAF and NCF, followed by a slight progressive increase for the rest of the time intervals. The lower residual Pb concentrations were obtained using NCF. CFA produced a steep decrease in Pb concentration within the first 10 min, followed by a progressive increase between 10 and 45 min, and a new decrease between 45 min and 2 h, with slight concentration fluctuations for the rest of the time intervals. The addition of NC and NCZ produced a steep decrease in Pb concentration within the first 5 min, followed by a very stable behaviour and a progressive decrease between 5 and 30 min using NC and NCZ, respectively; a sudden increase occurred between 30 min and 1 h, followed by a new decrease between 1 and 2 h, with slight concentration fluctuations for the rest of the time intervals.

In the case of As (Fig. 4(e)), CFAF and NCF produced a steep decrease during the first 5 min, after which plateau values were reached with very low residual concentrations (around 1 ppm) for the rest of the time intervals, with an almost complete removal. NCZ produced a steep decrease in As concentration during the first 45 min, with considerable inconsistency in concentration as indicated by fluctuations in the plot; NCZ shows a lower efficiency than that shown by faujasite, The addition of CFA and NC produced a steep decrease in As concentration within the first 5 min, followed by a very stable behaviour for the rest of the time intervals, although the CFA produced a sudden increase at 45 min. All sorbents showed a very slight progressive increase after 2 h of reaction.

Cu concentration is illustrated in Fig. 4(f) and is characterized by a steep increase within the first 5 min, using all sorbents, which continued after 10 min, except when CFA (small

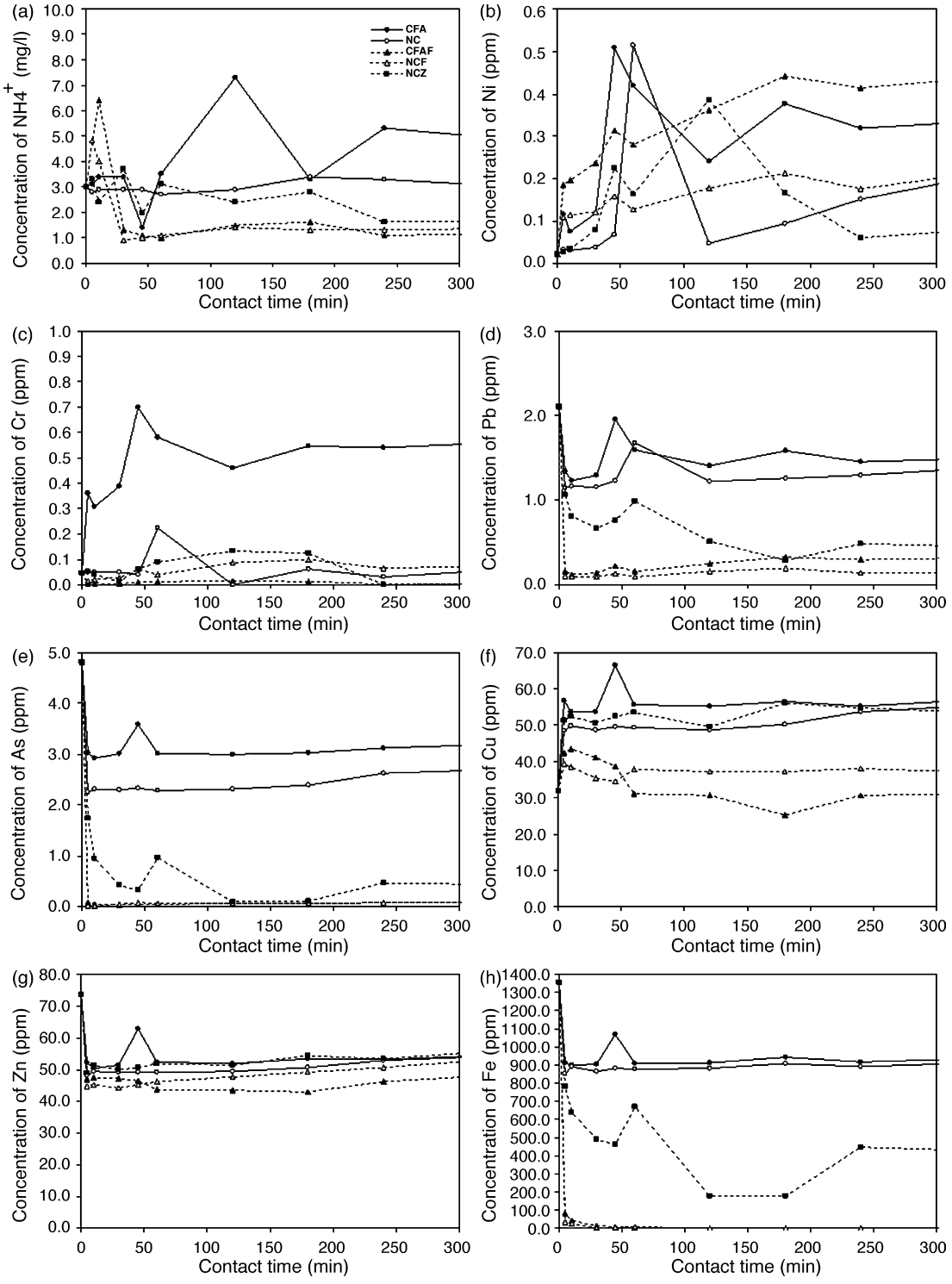

Fig. 4. Variation of concentration of (a) ammonium and (b–h) metals as a function of time during the sorption batch experiments with starting pH of 1.96 and EC of 3.77 mS/cm and sorbent:AMD mixture of 0.25 g/20 ml.

decrease) and NCF were added. CFAF produced a progressive decrease up to 3 h, followed by a new increase between 3 and 4 h. However, the trend after 1 h shows an almost stable behaviour. NCF produced also a progressive decrease up to 45 min, followed by an increase between 45 and 60 min, and then stabilized for the rest of the time intervals. NCZ produced slight concentration fluctuations. The addition of CFA and NC promoted a very stable behaviour of the Cu concentration, except by a significant fluctuation in concentration observed at 45 min using CFA and a slight progressive increase after 2 h using NC. The addition of CFA and NC promoted a very stable behaviour of the Cu concentration, except by a significant fluctuations in concentration observed at 45 min using CFA and a slight progressive increase after 2 h using NC. For all investigated materials, Cu

concentrations after sorbent:AMD interaction are higher than those contained originally in the raw AMD, which can also be explained by dissolution of the sorbents releasing Cu.

All sorbents produced similar trends of Zn (Fig. 4(g)) with an abrupt decrease within the first 5 min, reaching a very stable behaviour, except by CFA, which produced a sudden increase at 45 min. In general, Zn concentration tends to slightly increase at longer reaction time, particularly after 2 h.

In the case of Fe (Fig. 4(h)), CFAF and NCF produced a steep decrease during the first 5 min, followed by a progressive decrease up to 1 h, after which plateau values were reached with very low residual concentrations (around 1 ppm) for the rest of the time intervals, with an almost complete removal. NCZ showed a lower efficiency than that shown by faujasite, producing a steep decrease within the first 5 min, followed by a progressive increase up to 45 min; then, an abrupt increase was observed at 1 h, followed by a new decrease at 2 h, decreasing again for the rest of the time intervals. Therefore, this Fe trend showed an inconsistent behaviour in concentration characterized by significant concentration fluctuations. The addition of CFA and NC produced a steep decrease within the first 5 min, tending to stabilize for the rest of the time intervals, except by an abrupt increase in concentration observed at 45 min using CFA.

Based on the inherit alkalinity, induced by the alkaline activation of the raw materials, a higher pH was obtained upon zeolite addition. However, in conditions where the ion exchange process occurs in considerably alkaline pH ranges, the precipitation of certain solid phases on the surface of the ion exchanger may be induced and as such, they can act as crystallization seeds for the subsequent precipitation of the counter ion [28]. The result would be the enhancement of the metal uptake by the ion exchanger and this is what probably occurs during experiments with inorganic exchangers, such as the ones synthesized in this study. We can conclude that the main mechanism for metal uptake is precipitation and not sorption and the increase in pH with the addition of the sorbents decreases the metal concentrations probably due to precipitation on the surface of the sorbents. The process of precipitation works on the basis that the pH is reached at which the metals attain their minimum solubility and as such, precipitate out [28]. However, in spite each metal portray its own minimum solubility at its own characteristic pH, the pH required to precipitate most metals from water ranges from pH 6 to 9 (except for Fe, which precipitates at pH > 3.5), thus if sufficient alkaline material is added, such that the pH is raised up to 9, most of the metals will be hydrolyzed and precipitated [34].

3.3.4. Effect of sorbent dosage

A sorbent:AMD mixture of 1 g/20 ml was used to establish the effect of sorbent dosage, with an increase of pH in the batch experiments occurred after 24 h of contact time, with final pH values from 4.20 to 9.43, except when NC was used (pH 1.85). NCF was selected to develop an additional batch reaction test to evaluate the removal of heavy metals and ammonium because it produced the highest pH (9.43). Fig. 5 illustrates the trends of pH and electrical conductivity as well as the ammonium concentrations in AMD treated with NCF. The kinetics of the neutralization reaction is initially very rapid, with the pH (Fig. 5(a)) increasing rapidly from 1.96 to 7.70 within the first 5 min on contact with NCF, which is probably the result of the free CaO present in the faujasite framework. The reaction rate decreases as equilibrium is approached, with an apparent equilibrium pH of 8.34 being reached within 1 h. The pH increase can be also associated to dissolution of the sorbent during the shaking process. However, a final pH similar to that obtained in our batch experiments has been attributed to hydrolysis of zeolites as well as cationic exchange [35]. According to Ouki and Kavannagh [36] and Pitcher et al. [37], the pH increase is almost unavoidable in a zeolite heavy metal system. The electrical conductivity (Fig. 5(a)) also shows an abrupt increase from 3.77 to 9.42 mS/cm within the first 5 min, which becomes stable after 1 h of contact time. The ammonium concentration (Fig. 5(b)) shows a significant fluctuation during the first hour; a steep decrease from 3.0 to 0.30 mg/l of ammonium was observed within the first 5 min, with a progressive increase from 0.30 to 0.90 mg/l of ammonium between 5 and 45 min, finally decreasing with contact time, although a complete removal of ammonium was obtained only after 24 h. Fig. 6 illustrates the trends of heavy metal concentrations in AMD treated with NCF, which indicates that during the first 5 min an abrupt decrease in all the

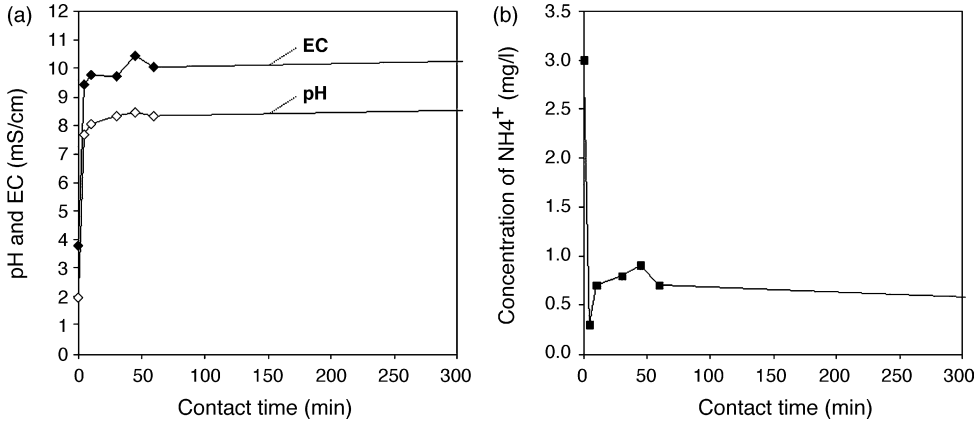

Fig. 5. Variation of (a) pH and electrical conductivity and (b) ammonium concentration as a function of time during the sorption batch experiments (NCF:AMD mixture of 1 g/20 ml) with starting pH of 1.96 and EC of 3.77 mS/cm.

analysed elements occurred, except Ni and Cr, which showed a very small increase. Then, an abrupt increase in Zn and Cu, with a progressive decrease and increase in Pb and Ni, respectively, was observed between 5 and 10 min, with Fe and As keeping constant. Cr displayed a very small decrease during this contact time. A steep decrease in Zn and Cu, with increasing Pb, Ni, Cr and As, occurred between 10 and 30 min, with Fe keeping constant. A progressive increase in Pb and As, with a decrease in Ni, Zn and Cr, occurred between 30 and 45 min. Finally, between 45 and 60 min a decrease in Pb and As, a very small decrease in Zn and Cr, and an increase in Ni, was observed. With contact time the concentration levels decreased to the lower values. In general, all metals showed a very steep concentration decrease during the first 5 min, reaching plateau values with very low residual concentrations for the rest of the time intervals, although without a complete removal, with Pb and Ni showing slight concentration fluctuations during the first hour. The plots in Fig. 6 show the fact that removal was quite favourable in terms of Fe, Zn, Cu, As and Pb, taking into account that very low residual concentrations were obtained after equilibration with NCF. Cr and Ni maintained fairly stable, showing very low concentrations. pH has a very important role in the sorption/removal of the contaminants, probably due to the charge developed on the surfaces of the adsorbent as the pH increased. On the other hand, a higher adsorbent ratio showed a better efficiency in the removal of contaminants.

3.3.5. *pH versus dissolved metal content*

The relationship between pH and the dissolved metal content in AMD can be summarized using 'Ficklin' diagrams [38–41], as shown in Fig. 7. These plots are very useful to carry out an initial prediction of the potential impact from mining sulphide-bearing mineral deposits, enabling an assessment of correlations between particular mineral-deposit types and the observed metal, metalloid, pH and sulphate chemistry in the drainage [42]. However, in this study we use the Ficklin diagrams to make a relationship between the metal concentration in treated AMDs and that corresponding to natural AMDs associated to different mineral assemblages and geological conditions. The raw AMD is characterized by high acid values of pH and extreme metal concentrations (Fig. 7) and its plot falls within the field typically associated with pyrite–enargite–chalcocite–covelline in acid altered rocks [40]. Similar results were observed when AMD was treated with CFA and NC (Fig. 7(a)) or with NCZ (Fig. 7(b)), which are characterized by high acid values of pH and extreme metal concentrations, with the cluster of points being equivalent to AMDs associated with pyrite–enargite–chalcocite–covelline in acid altered rocks. When CFAF (Fig. 7(c)) and NC (Fig. 7(d)) were used during AMD treatment, moderate acid values of pH and extreme to high metal concentrations were obtained, which is equivalent to AMDs associated with pyrite–sphalerite–galena–chalcopyrite in carbonate-poor rocks. The effect of sorbent dosage is illustrated

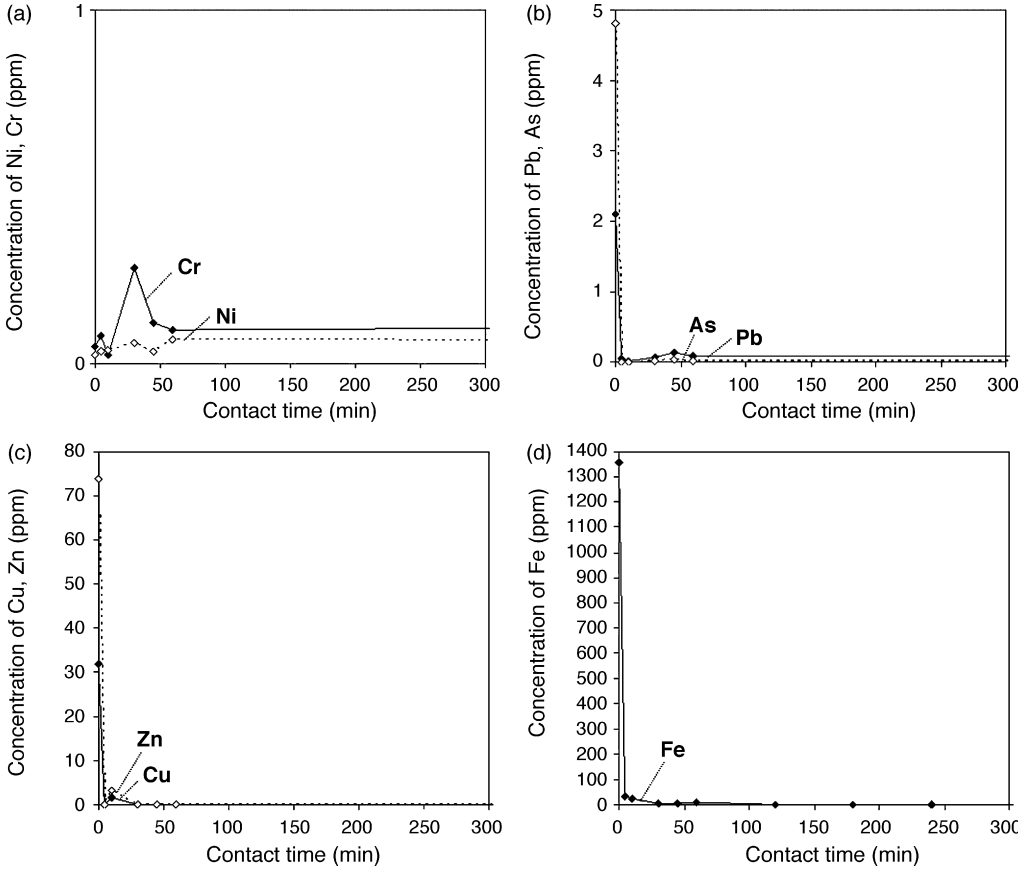

Fig. 6. Variation of heavy metal concentration as a function of time during the sorption batch experiments (NCF:AMD mixture of 1 g/20 ml) with starting pH of 1.96 and EC of 3.77 mS/cm.

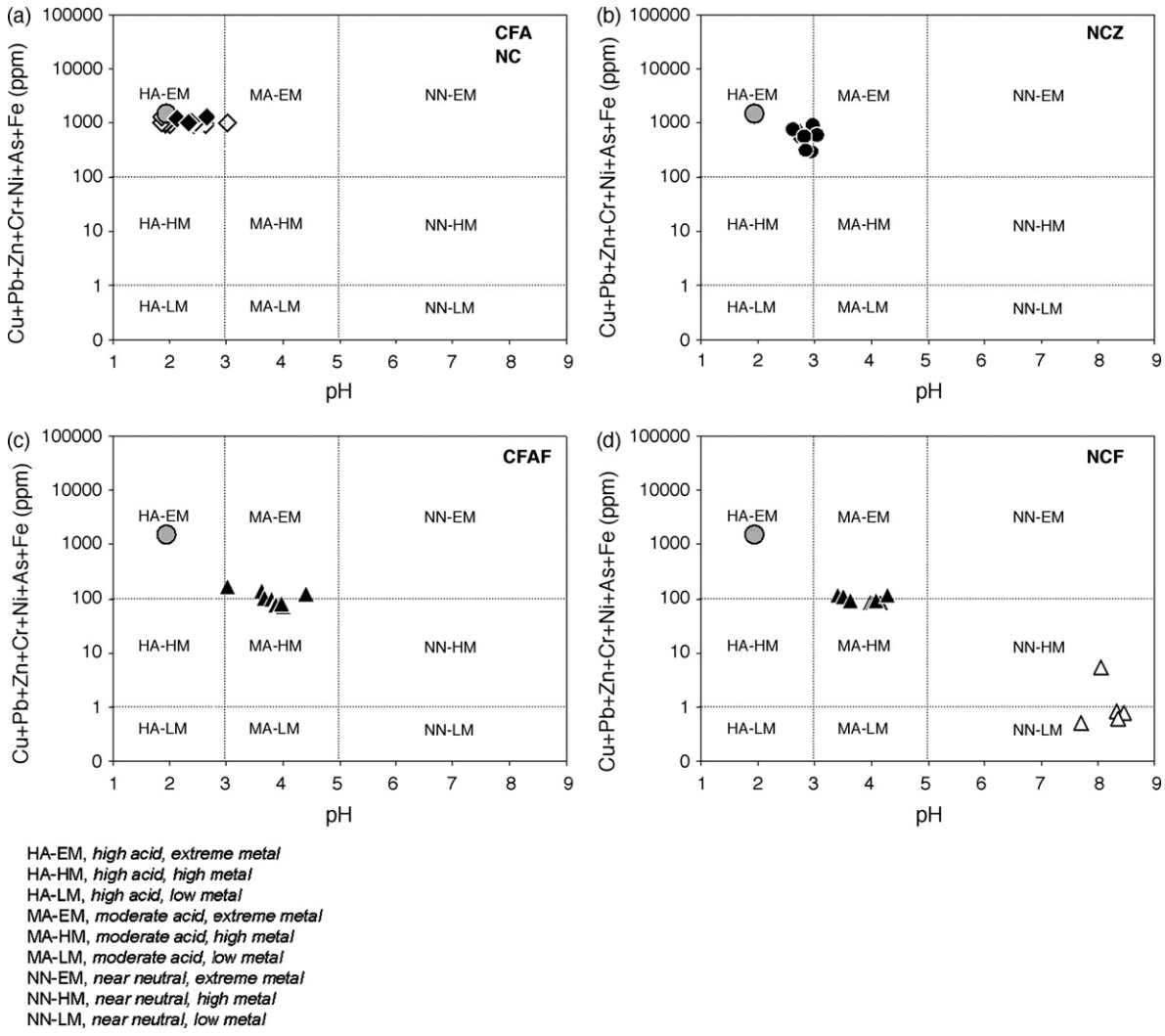

Fig. 7. Ficklin diagrams showing the sum of aqueous base metal concentrations in AMD treated with (a) CFA and NC, (b) NCZ, (c–d) CFAF and NCF, respectively. AMD plots (grey circle) indicate the starting heavy metal concentration and pH, whereas the treated AMD data using a sorbent:AMD mixture of 0.25 g/20 ml are indicated by black rombs (CFA); open rombs (NC); black circles (NCZ); black triangles (CFAF and NCF). Open triangles indicate a NCF:AMD mixture of 1 g/20 ml.

in Fig. 7(d). A NCF:AMD mixture of 1 g/20 ml produced mainly near neutral pH and low metal concentrations, although after 5 min of reaction a near neutral pH and a high metal concentration was obtained, which is equivalent to AMDs associated with pyrite-poor sphalerite-galena veins and replacements in carbonate rocks or with pyrite-poor gold-telluride veins and breccias with carbonates. Therefore, the use of a higher sorbent dosage in the treatment of AMD promoted the increase of the pH and the reduction of metal concentration.

4. Conclusions

In this study, CFA, NC and synthetic zeolites were investigated in batch experiments as potential sorbents for treatment of AMD at a starting pH of 1.96, which changed after 24 h to 2.66 and 4.20 (CFA), 1.86 and 1.85 (NC), 4.42 and 8.41 (CFAF), 4.29 and 9.43 (NCF) and 2.86 and 3.89 (NCZ), with pH values increasing with sorbent dosage, except when NC was used, which suggests that with sufficient reaction time (24 h), the pH is strongly affected by the sorbent material rather than the AMD composition and particularly with a higher sorbent dosage. There are two competing processes here, release of alkalinity from sorbents and removal of acidity from AMD components, at higher sorbent dosage the acidity from AMD components is overwhelmed and pH is bound to increase while with lower sorbent dosage the alkalinity from the sorbent is overwhelmed by the acidity from the AMD components and the pH remains low. Our experimental data reveal that the heavy metal removal will depend on the sorbent material and the applied dosage; NC and probably CFA did not show good efficiency as sorbents to neutralize the AMD, but their synthesis products are beneficial products as ion exchangers in removing acidity, Fe, Zn and Cu from AMD. In addition to cation exchange reactions, precipitation of hydroxide species (mainly of Fe) also played an important role in the sorption and coprecipitation, and thus immobilization of metals in the batch experiments carried out. The results of the absorption experiments suggest that faujasite can be applied in wastewater treatment as an immobilizer of pollutants. Selectivity of faujasite for metal removal was, in decreasing order, Fe > As > Pb > Zn > Cu > Ni > Cr. From the

above results, we have demonstrated that faujasite was effective in reducing the Fe, As and Pb concentration, indicating the complete removal of Fe and As with a strongly irreversible character and not a complete removal of Pb, in spite of the dosage of sorbent applied during AMD treatment. Cu and Zn were partially removed when 1 g of sorbent was reacted with the AMD. Ni shows a small progressive increase and displays a similar trend to Pb, except when NCZ was used. The efficiency in the removal of ammonium was poor. However, the reaction between synthetic zeolites and AMD after 24 h of contact time produced the lower ammonium concentrations. NCF produced a complete removal of ammonium was obtained after 24 h of contact time when a dosage of 1 g was used. In general, the different sorbents contain considerable amounts of accessory phases that partly dissolve during the batch reaction, which may explain the sudden increase or decrease in metal concentration and therefore, the release rate of these elements is controlled by the dissolution of the sorbent. Our results can be applied in waste management scenarios, particularly in AMD treatment. However, it will be necessary to design and execute some more detailed experiments to explore further application of the adsorbents for clean-up of the AMD, which can be treated at the mine to some degree, usually by neutralisation at source by limestone, settling and tailings ponds or wetlands, although this process will not be ever fully efficient and accidents with the treatment system are inevitable.

Acknowledgments

This research was supported by the Programme Alban, 'the European Union Programme of High Level Scholarships for Latin America', Scholarship No. E05D060429CO, and the Universidad Industrial de Santander (a remunerated commission) for funding C. Ríos, and has benefited from research facilities provided by the School of Applied Sciences at the University of Wolverhampton. We acknowledge Dr. David Townrow and Mrs. Barbara Hodson for assistance with XRD and SEM data acquisition, respectively. We are thankful to Dr. Wilson Gitari and Ms. Leslie Petrik from the Environmental and Nano sciences group, University of the Western Cape, South Africa, for their useful comments and suggestions.

References

[1] N.M. Dubrovsky, J.A. Cherry, E.J. Reardon, A.J. Vivyurka, Geochemical evolution of inactive pyritic tailings in Elliott Lake uranium district, Can. Geotech. J. 22 (1985) 110–128.
[2] D.G. Feasby, M. Blanchette, G. Tremblay, L.L. Sirois, The mine environment neutral drainage program, in: Proceedings of the 2nd International Conference on the Abatement of Acidic Drainage, vol. 1, Montreal, PQ, 1991, pp. 1–26.
[3] E.M.R. Kuhn, Microbiology of fly ash-acid mine drainage co-disposal processes, Master thesis, University of the Western Cape, 2005.
[4] P.C. Singer, W. Stumm, Acidic mine drainage: the rate determining step, Science 167 (1970) 1121–1123.
[5] L.M. Prescott, J.P. Harley, D.A. Klein, Microbiology, Fourth ed., McGraw-Hill, New York, 1999.
[6] F.H. Pearson, A.J. McDonnell, Use of crushed limestone to neutralise acid wastes, J. Environ. Eng. Div. 101 (1975) 139–158.
[7] D. Feng, C. Aldrich, H. Tan, Treatment of acid mine water by use of heavy metal precipitation and ion exchange, Miner. Eng. 13 (2000) 623–642.
[8] D. Mohan, S. Chander, Single component and multi-component adsorption of metal ions by activated carbons, Colloids Surf. A 177 (2001) 183–196.
[9] M.M.G. Chartrand, N.J. Bunce, Electrochemical remediation of acid mine drainage, J. Appl. Electrochem. 33 (2003) 259–264.
[10] S. Santos, R. Machado, M.J.N. Correia, Treatment of acid mining waters, Miner. Eng. 17 (2004) 225–232.
[11] O. Gibert, J. de Pablo, J.L. Cortina, C. Ayora, Municipal compost-based mixture for acid mine drainage bioremediation: metal retention mechanisms, Appl. Geochem. 20 (2005) 1648–1657.
[12] O. Gibert, J. de Pablo, J.L. Cortina, C. Ayora, Sorption studies of Zn(II) and Cu(II) onto vegetal compost used on reactive mixtures for in situ treatment of acid mine drainage, Water Res. 39 (2005) 2827–2838.
[13] D.B. Johnson, K.B. Hallberg, Acid mine drainage remediation options: a review, Sci. Total Environ. 338 (2005) 3–14.
[14] B.J. Wattena, P.L. Sibrella, M.F. Schwartzb, Acid neutralization within limestone sand reactors receiving coal mine drainage, Environ. Pollut. 137 (2005) 295–304.
[15] X. Wei, R.C. Viadero Jr., K.M. Buzby, Recovery of iron and aluminium from acid mine drainage by selective precipitation, Environ. Eng. Sci. 22 (2005) 745–755.
[16] M. Kalin, A. Fyson, W.N. Wheeler, The chemistry of conventional and alternative treatment systems for the neutralization of acid mine drainage, Sci. Total Environ. 366 (2006) 395–408.
[17] D. Mohan, S. Chander, Removal and recovery of metal ions from acid mine drainage using lignite—a low cost sorbent, J. Hazard. Mater. B137 (2006) 1545–1553.
[18] N. Moreno, X. Querol, C. Ayora, C.F. Pereira, M. Janssen-Jurkovičová, Utilization of zeolites synthesized from coal fly ash for the purification of acid mine waters, Environ. Sci. Technol. 35 (2001) 3526–3534.
[19] N. Moreno, X. Querol, C. Ayora, A. Alastuey, C. Fernández-Pereira, M. Janssen-Jurkovičová, Potential environmental applications of pure zeolitic material synthesized from fly ash, J. Environ. Eng. 127 (2001) 994–1002.
[20] L.F. Petrik, R.A. White, M.J. Klink, V.S. Somerset, C.L. Burgers, M.V. Fey, Utilization of South African fly ash to treat acid coal mine drainage, and production of high quality zeolites from the residual solids, in: Proceedings of the International Ash Utilization Symposium, Centre for Applied Energy Research, University of Kentucky, 2003, pp. 1–26.
[21] U. Wingenfelder, C. Hansen, G. Furrer, R. Schulin, Removal of heavy metals from mine waters by natural zeolites, Environ. Sci. Technol. 39 (2005) 4606–4613.
[22] M.W. Gitari, L.F. Petrik, O. Etchebers, D.L. Key, E. Iwuoha, C. Okujeni, Treatment of acid mine drainage with fly ash: removal of major contaminants and trace elements, J. Environ. Sci. Health A: Tox. Hazard. Subst. Environ. Eng. 41 (2006) 1729–1747.
[23] R. Pérez-López, J.M. Nieto, G. Ruiz de Almodóvar, Utilization of fly ash to improve the quality of the acid mine drainage generated by oxidation of a sulphide-rich mining waste: column experiments, Chemosphere 67 (2007) 1637–1646.
[24] R. Pérez-López, J. Cama, J.M. Nieto, C. Ayora, The iron-coating role on the oxidation kinetics of a pyritic sludge doped with fly ash, Geochim. Cosmochim. Acta 71 (2007) 1921–1934.
[25] S.V. Vassilev, C.G. Vassileva, A new approach for the classification of coal fly ashes based on their origin, composition, properties, and behaviour, Fuel 86 (2007) 1490–1512.
[26] S. Rayalu, S.U. Meshram, M.Z. Hasan, Highly crystalline zeolites from fly ash, J. Hazard. Mater. B77 (2000) 123–131.
[27] N.Z. Misak, Some aspects of the application of adsorption isotherms to ion exchange reactions, React. Funct. Polym. 43 (2000) 153–164.
[28] N.R. Hendricks, The application of high capacity ion exchange adsorbent material, synthesized from fly ash and acid mine drainage, for the removal of heavy and trace metals from secondary co-disposed process waters, Master's thesis, University of the Western Cape, 2005.
[29] V.L. Snoeyink, D. Jenkis, Water Chemistry, John Wiley & Sons, Inc., New York, 1980.

[30] T.R. Smith, T.P. Wilson, F.N. Ineman, The relationship of iron bacteria geochemistry to trace metal distribution in an acid mine drainage system, NE Ohio, Geol. Soc. Am. Abstracts with Programs 23 (1991), p. 61.
[31] W. Uhlmann, H. Buttcher, O. Totsche, C.E.W. Steinberg, Buffering of acidic mine lakes: the relevance of surface exchange and solid bound sulphate, Mine Water Environ. 23 (2004) 20–27.
[32] W. Stumm, G.F. Lee, Oxygenation of ferrous iron, Ind. Eng. Chem. 53 (1961) 143–146.
[33] J. Peric, M. Trigo, N.V. Medvidović, Removal of zinc, copper and lead by natural zeolite—a comparison of adsorption isotherms, Water Res. 38 (2004) 1893–1899.
[34] V.P. Evangelou, Y.L. Zhang, A review: pyrite oxidation mechanisms and acid mine drainage prevention, Crit. Rev. Env. Sci. Technol. 25 (1995) 141–199.
[35] H. Genç-Fuhrman, P.S. Mikkelsen, A. Ledin, Simultaneous removal of As, Cd, Cr, Cu, Ni and Zn from stormwater: experimental comparison of 11 different Sorbents, Water Res. 41 (2007) 591–602.
[36] S.K. Ouki, M. Kavannagh, Performance of natural zeolites for the treatment of mixed metal-contaminated effluents, Waste Manage. Res. 15 (1997) 383–394.
[37] S.K. Pitcher, R.C.T. Slade, N.I. Wards, Heavy metal removal from motorway stormwater using zeolites, Sci. Total Environ. 334-335 (2004) 161–166.
[38] W.H. Ficklin, G.S. Plumlee, K.S. Smith, J.B. McHugh, Geochemical classification of mine drainages and natural drainages in mineralized areas, in: Y.K. Kharaka, A.S. Maest (Eds.), Proceedings of the 7th International Symposium on Water Rock Interaction, Park City, Utah, 1992, pp. 381–384.
[39] G.S. Plumlee, K.S. Smith, E.L. Mosier, W.H. Ficklin, M.R. Montour, P. Briggs, A. Meier, Geochemical processes controlling acid-drainage generation and cyanide degradation at Summitville, in: H.H. Posey, J.A. Pendleton, D.J.A. Van Zyl (Eds.), Proceedings of the Summitville Forum'95, Colorado Geol. Surv. Spec. Pub. 38, Colorado, 1995, pp. 23–34.
[40] R.R. Seal II, N.K. Foley, R.B. Wanty, Introduction to geoenvironmental models of mineral deposits, in: R.R. Seal II, N.K. Foley (Eds.), Progress on Geoenvironmental Models for Selected Mineral Deposit Types, US Geol. Surv. Open File Rep. 02-195, 2002, pp. 1–7.
[41] A.J. Desbarats, G.C. Dirom, Temporal variations in the chemistry of circum-neutral drainage from the 10-Level portal, Myra Mine, Vancouver Island, British Columbia, Appl. Geochem. 22 (2007) 415–435.
[42] R.J. Bowell, J.V. Parshley, Control of pit-lake water chemistry by secondary minerals, Summer Camp pit, Getchell mine, Nevada, Chem. Geol. 215 (2005) 373–385.